Author(s): Hyvärinen, Juhani; Suhonen, Jouni

Title: Analysis of the Intermediate-State Contributions to Neutrinoless Double β− Decays

Year: 2016

Version:

Please cite the original version:

Hyvärinen, J., & Suhonen, J. (2016). Analysis of the Intermediate-State Contributions to Neutrinoless Double β− Decays. Advances in High Energy Physics, 2016, Article 4714829. https://doi.org/10.1155/2016/4714829

Hindawi Publishing Corporation
Advances in High Energy Physics
Volume 2016, Article ID 4714829, 13 pages
http://dx.doi.org/10.1155/2016/4714829

Research Article

Analysis of the Intermediate-State Contributions to Neutrinoless Double β^- Decays

Juhani Hyvärinen and Jouni Suhonen

Department of Physics, University of Jyvaskyla, P.O. Box 35, 40014 Jyvaskyla, Finland

Correspondence should be addressed to Juhani Hyvärinen; juhani.t.hyvarinen@student.jyu.fi

Received 1 April 2016; Accepted 26 May 2016

Academic Editor: Luca Stanco

A comprehensive analysis of the structure of the nuclear matrix elements (NMEs) of neutrinoless double beta-minus ($0\nu\beta^-\beta^-$) decays to the 0^+ ground and first excited states is performed in terms of the contributing multipole states in the intermediate nuclei of $0\nu\beta^-\beta^-$ transitions. We concentrate on the transitions mediated by the light (l-NMEs) Majorana neutrinos. As nuclear model we use the proton-neutron quasiparticle random-phase approximation (pnQRPA) with a realistic two-nucleon interaction based on the Bonn one-boson-exchange G matrix. In the computations we include the appropriate short-range correlations, nucleon form factors, and higher-order nucleonic weak currents and restore the isospin symmetry by the isoscalar-isovector decomposition of the particle-particle proton-neutron interaction parameter g_{pp}.

1. Introduction

Thanks to neutrino-oscillation experiments much is known about the basic properties of the neutrino concerning its mixing and squared mass differences. What is not known is the absolute mass scale, the related mass hierarchy, and the fundamental nature (Dirac or Majorana) of the neutrino. This can be studied by analyzing the neutrinoless double beta ($0\nu2\beta$) decays of atomic nuclei [1–4] through analyses of the participating nuclear matrix elements (NMEs). The $0\nu2\beta$ decays proceed by virtual transitions through states of all multipoles J^π in the intermediate nucleus, J being the total angular momentum and π being the parity of the intermediate state. Most of the present interest is concentrated on the double beta-minus variant ($0\nu\beta^-\beta^-$ decay) of the $0\nu2\beta$ decays due to their relatively large decay energies (Q values) and natural abundancies.

In this work we concentrate on analyses of the intermediate contributions to the $0\nu\beta^-\beta^-$ decays for the $0^+ \rightarrow 0^+$ ground-state-to-ground-state and ground-state-to-excited-state transitions in nuclear systems of experimental interest. We focus on the light Majorana neutrino mediated transitions by taking into account the appropriate short-range nucleon-nucleon correlations [5] and contributions arising from the induced currents and the finite nucleon size [6]. There are several nuclear models that have recently been used to compute the $0\nu\beta^-\beta^-$ decay NMEs (see, e.g., the extensive discussions in [3, 7–11]). However, the only model that avoids the closure approximation and retains the contributions from individual intermediate states is the proton-neutron quasiparticle random-phase approximation (pnQRPA) [7, 12–14].

Some analyses of the intermediate-state contributions within the pnQRPA approach have been performed in [12, 13, 15, 16] and recently quite extensively in [17]. In [17] an intermediate multipole J^π decomposition was done for decays of ^{76}Ge, ^{82}Se, ^{96}Zr, ^{100}Mo, ^{110}Pd, ^{116}Cd, ^{124}Sn, ^{128,130}Te, and ^{136}Xe to the ground state of the respective daughter nuclei. In this paper we extend the analysis of [17] to a more detailed scrutiny of the intermediate contributions to the $0\nu\beta^-\beta^-$ decay NMEs of the above-mentioned nuclei. We also extend the scope of [17] by considering transitions to the first 0^+ excited states in addition to the ground-state-to-ground-state transitions.

2. Theory Background

In this section a very brief introduction to the computational framework of the present calculations is given. The present analyses on ground-state-to-ground-state decays are based on the calculations done in [17]. Details considering the excited-state decays are given in a future publication. We assume here that the $0\nu\beta^-\beta^-$ decay proceeds via the light Majorana neutrino so that the inverse half-life can be written as

$$\left[t_{1/2}^{(0\nu)}\left(0_i^+ \longrightarrow 0_f^+\right)\right]^{-1} = g_{\mathrm{A}}^4 G_{0\nu}\left|M^{(0\nu)}\right|^2 \left|\langle m_\nu\rangle\right|^2, \quad (1)$$

where $G_{0\nu}$ is a phase-space factor for the final-state leptons defined here without the axial vector coupling constant g_{A}. The quantity $\langle m_\nu\rangle$ denotes the neutrino effective mass and describes the physics beyond the standard model [17]. The quantity $M^{(0\nu)}$ is the light neutrino nuclear matrix element (l-NME). The nuclear matrix element can be decomposed into Gamow-Teller (GT), Fermi (F), and tensor (T) contributions as

$$M^{(0\nu)} = M_{\mathrm{GT}}^{(0\nu)} - \left(\frac{g_{\mathrm{V}}}{g_{\mathrm{A}}}\right)^2 M_{\mathrm{F}}^{(0\nu)} + M_{\mathrm{T}}^{(0\nu)}, \quad (2)$$

where g_{V} is the vector coupling constant.

Each of the NMEs K = GT, F, and T in (2) can be decomposed in terms of the intermediate multipole contributions J^π as

$$M_K^{(0\nu)} = \sum_{J^\pi} M_K^{(0\nu)}\left(J^\pi\right), \quad (3)$$

where each multipole contribution is, in turn, decomposed in terms of the two-particle transition matrix elements and one-body transition densities as

$$\begin{aligned} M_K^{(0\nu)}\left(J^\pi\right) = {} & \sum_{k_1,k_2,J'} \sum_{pp'nn'} (-1)^{j_n+j_{p'}+J+J'} \sqrt{2J'+1} \\ & \times \begin{Bmatrix} j_p & j_n & J \\ j_{n'} & j_{p'} & J' \end{Bmatrix} \left(pp' : J' \left\| \mathcal{O}_K \right\| nn' : J'\right) \\ & \times \left(0_f^+ \left\| \left[c_{p'}^\dagger \tilde{c}_{n'}\right]_J \right\| J_{k_1}^\pi\right) \left\langle J_{k_1}^\pi \mid J_{k_2}^\pi \right\rangle \left(J_{k_2}^\pi \left\| \left[c_p^\dagger \tilde{c}_n\right]_J \right\| 0_i^+\right), \end{aligned} \quad (4)$$

where k_1 and k_2 label the different pnQRPA solutions for a given multipole J^π and the indices p, p', n, n' denote the proton and neutron single-particle quantum numbers. The operators $\mathcal{O}_K$ inside the two-particle matrix element contain the neutrino potentials for the light Majorana neutrinos, the characteristic two-particle operators for the different K = GT, F, T and a function taking into account the short-range correlations (SRC) between the two decaying neutrons in the mother nucleus of $0\nu\beta^-\beta^-$ decay [17]. The final 0^+ state, 0_f^+, can be either the ground state or an excited state of the $0\nu\beta^-\beta^-$ daughter nucleus, and the overlap factor between the two one-body transition densities helps connect the corresponding intermediate J^π states emerging from the pnQRPA calculations in the mother and daughter nuclei.

As mentioned before, our calculations contain the appropriate short-range correlators, nucleon form factors, and higher-order nucleonic weak currents. In addition, we decompose the particle-particle proton-neutron interaction strength parameter g_{pp} of the pnQRPA into its isoscalar ($T = 0$) and isovector ($T = 1$) components and adjust these components independently as described in [17]: the isovector component is fixed such that the NME of the two-neutrino double beta-decay ($2\nu\beta^-\beta^-$) vanishes and the isospin symmetry is thus restored for both the $2\nu\beta^-\beta^-$ and $0\nu\beta^-\beta^-$ decays. The isoscalar component, in turn, is fixed such that the measured half-life of the $2\nu\beta^-\beta^-$ decay is reproduced. The resulting values of both components of g_{pp} are shown in Table I of [17]. The details of the chosen valence spaces and the determination of the other Hamiltonian parameters are presented in [17]. We further note that in [17] two sets of NME computations, related to the value of the axial vector coupling g_{A}, were performed: first with the quenched value $g_{\mathrm{A}} = 1.00$ and then with the bare value $g_{\mathrm{A}} = 1.26$. In both computations the value of g_{A} was fixed first. After this the Hamiltonian parameters were adjusted by using the experimental data, as briefly described above and more thoroughly in [17].

3. Results and Discussion

In this section we discuss and present the results of our calculations. Presentation of the results follows top to bottom approach. First we analyze the multipole decompositions and total cumulative sums of the matrix elements. From these we can extract the most important multipole components and energy regions contributing to the NMEs. After this we continue and dissect the most important multipole components into contributions coming from different individual states of the $0\nu\beta\beta$ intermediate nucleus. Throughout these computations we have used a conservatively quenched value of the axial vector coupling $g_{\mathrm{A}} = 1.00$; that is, we use the pnQRPA parameters which are related to the first set of computations in [17] as was explained at the end of Section 2.

There has been a lot of discussion about the correct value of g_{A} in both the $2\nu\beta\beta$ and $0\nu\beta\beta$ decays lately. This is so due to the fact that a large portion of the theoretical half-life uncertainties are related to the present ambiguity in the value of g_{A}. In [9] the quenching of g_{A} was studied in the framework of IBM-2 and the interacting shell model (ISM). The effective g_{A} values were parametrized as $g_{\mathrm{A}}^{\mathrm{eff}} = 1.269A^{-0.18}$ (IBM-2) and as $g_{\mathrm{A}}^{\mathrm{eff}} = 1.269A^{-0.12}$ (ISM). These parametrizations were obtained by comparing the model calculations with experimental data on $2\nu\beta\beta$ decays. Further studies were performed within the framework of the pnQRPA by using the available Gamow-Teller beta-decay and $2\nu\beta\beta$ decay data in several publications (see [18] and the references therein). A wide systematic study of the quenching of g_{A} for Gamow-Teller beta decays was performed in [18]. Even the quenching related to spin-dipole 2^- states was studied in [19]. While the beta decays and $2\nu\beta\beta$ decays are low-energy processes with small momentum transfers, the $0\nu\beta\beta$ decay involves large momentum transfers and the thus

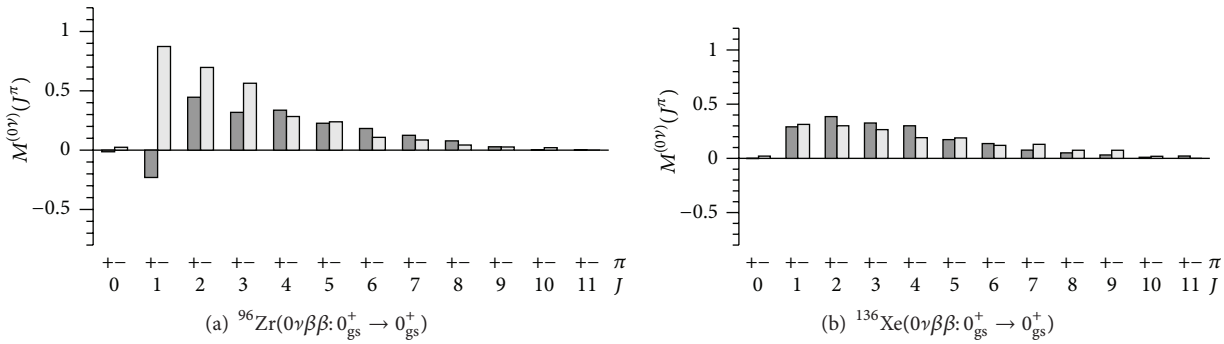

(a) ^{96}Zr($0\nu\beta\beta$: $0^+_{gs} \to 0^+_{gs}$) (b) ^{136}Xe($0\nu\beta\beta$: $0^+_{gs} \to 0^+_{gs}$)

Figure 1: Multipole decomposition of the l-NME for the nuclei ^{96}Zr and ^{136}Xe corresponding to the $0^+_{gs} \to 0^+_{gs}$ decay transitions.

activated high-energy and high-multipolarity intermediate states. For higher momentum transfers the effective g_A can be momentum-dependent [20] and different multipoles can be affected in different ways. At present there exists no known recipe on how to determine the value of g_A for the neutrinoless double beta decays, and that is why we have chosen in the present study to work with a moderately quenched value $g_A = 1.00$, assumed to be the same for all intermediate multipoles. We will study, however, the effect of changing the value of g_A to the characteristics of the intermediate-state contributions in Section 3.3.

3.1. Ground-State-to-Ground-State Transitions. Let us begin by considering the ground-state-to-ground-state decays mediated by light neutrino exchange. In Figures 1(a) and 1(b) we have plotted the multipole decomposition (3) of the l-NMEs corresponding to the $A = 96$ and 136 nuclear systems. For most nuclei considered in this work, the leading multipole component is 1^-. This is the case also for the nucleus ^{96}Zr shown in Figure 1(a). Most important contribution to the NMEs comes from the lowest multipole components $1^\pm - 4^\pm$. It can also be observed that the shape of the overall multipole distribution is leveled when going towards heavier nuclei. This can be seen by comparing the distribution of ^{96}Zr with the distribution of ^{136}Xe displayed in Figure 1(b).

Nuclei can be grouped into different types according to the shapes of their cumulative NME distributions. For $0^+_{gs} \to 0^+_{gs}$ transitions via light neutrino exchange, we can differentiate four types of nuclei. *Type 1*: nuclei belonging to this type are ^{76}Ge, ^{82}Se, ^{96}Zr, and ^{128}Te. Representative of this type, ^{76}Ge, is presented in Figure 2(a). Characteristic feature of the cumulative sum distribution belonging to type 1 is the strong drop in the value of the NME occurring between 12 and 17 MeV. Soon after this drop the NME saturates as can be seen from panel (a). *Type 2*: nuclei belonging to this type are ^{100}Mo and ^{110}Pd. Representative of this type, ^{110}Pd, is presented in Figure 2(b). Characteristic feature of this type is the large enhancement and almost immediate cancellation of this enhancement around 10 MeV. This produces a spike-like structure into the cumulative sum distribution as can be seen from panel (b). *Type 3*: nuclei belonging to type 3 are ^{116}Cd, ^{124}Sn, and ^{130}Te. Type 3 is represented by ^{124}Sn, shown in Figure 2(c). Characteristic features of this type are that there occurs neither sharp cancellation of the NME around 12–17 MeV, as in type 1, nor a spike like structure around 10 MeV, as in type 2. Value of the NME rather increases more or less smoothly to its highest value and then smoothly saturates to its final value around 20 MeV. *Type 4*: type 4 is special in a sense that it includes only one nucleus, ^{136}Xe. Cumulative sum of the NME for ^{136}Xe is shown in Figure 2(d). Characteristic feature of type 4 is that the lowest energy region, roughly between 0 and 1.5 MeV, contributes practically nothing to the value of the NME as can be noticed from panel (d).

Using the multipole decompositions, we have extracted the most important multipole components contributing to the light neutrino mediated ground-state-to-ground-state decays. These most important components can be divided into contributions coming from different energy levels of the $0\nu\beta\beta$ intermediate nucleus. These contributions are collected into Table 1 for $A = 76$–100 systems, into Table 2 for $A = 110$–124 systems, and into Table 3 for $A = 128$–136 systems. We see from the tables that often a very small set of states collects the largest part of a given multipole contribution to the NMEs. Also in some cases notable contributions are coming from high excitation energies, well above 10 MeV, like in the case of 1^- contributions for almost all nuclei, 1^+ contributions for ^{76}Ge, ^{82}Se, ^{110}Pd, ^{116}Cd, and ^{124}Sn, 2^+ contributions for ^{130}Te and ^{136}Xe, and a 3^- contribution for ^{124}Sn.

We notice a single-state dominance for the 2^- mode in nuclei ^{76}Ge, ^{82}Se, and ^{96}Zr. In [19] an analysis of the unique first forbidden single $\beta^\pm$ $2^- \to 0^+$ ground-state-to-ground-state transitions in the mass region $A = 72$–132 was performed. It was found that a strong renormalization of the axial vector 2^- single β matrix elements is needed to be able to explain the experimental transition rates. It was then speculated that the same kind of an effect may also appear in the $0\nu\beta\beta$ NMEs. This may have a large effect on the $0\nu\beta\beta$ transition rates due to the important contribution of the 2^- multipole to the $0\nu\beta\beta$ NMEs.

The energies of the intermediate states listed in Tables 1, 2, and 3 (and also those in Tables 4 and 5 for the transitions to the excited states) originate from pnQRPA calculations. Usually the pnQRPA cannot reproduce the fine details of

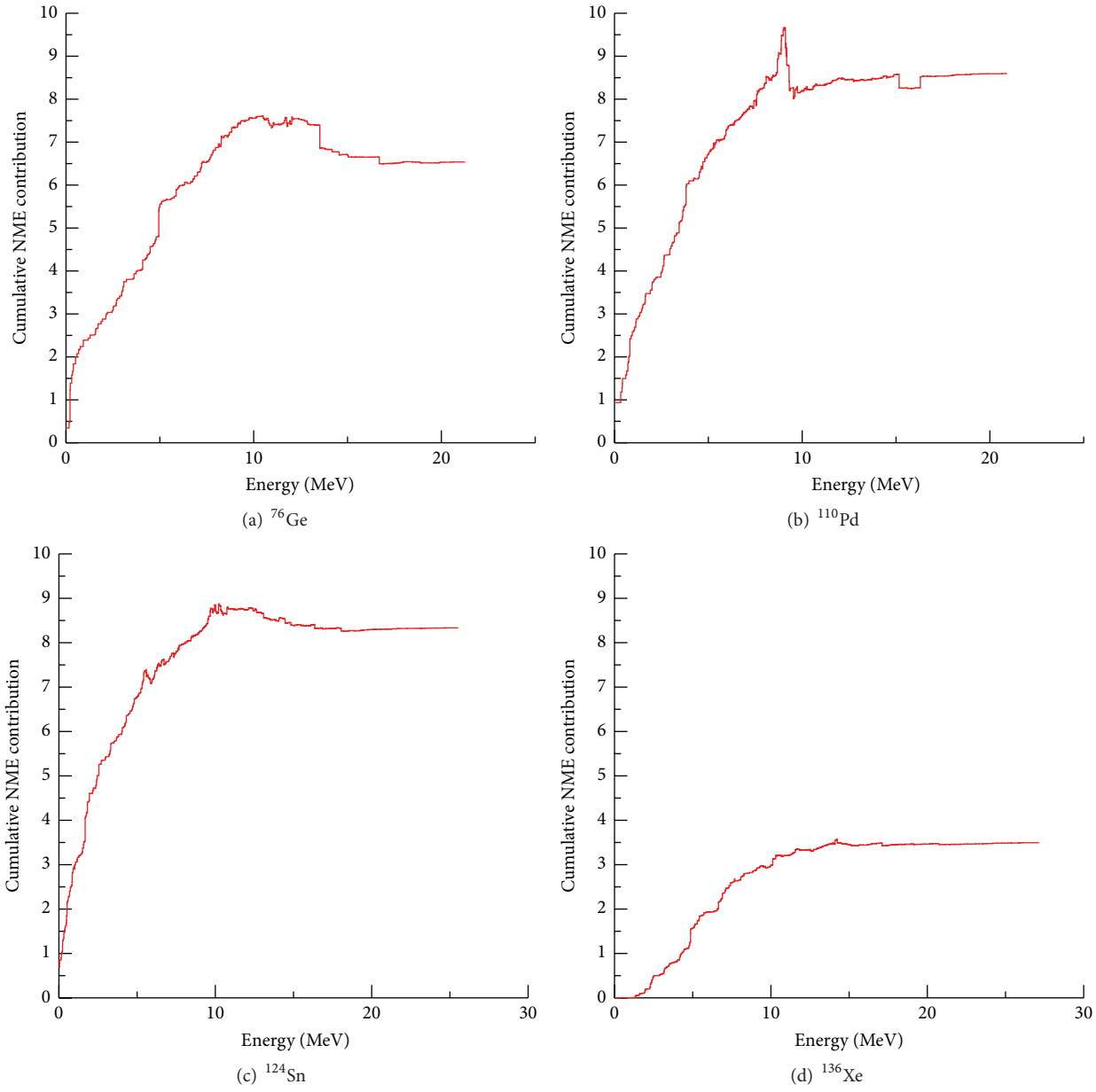

FIGURE 2: Cumulative values of the computed l-NMEs corresponding to the $0^+_{gs} \rightarrow 0^+_{gs}$ decay transitions for the nuclear systems $A = 76, 110, 124$ and 136. The horizontal axis gives the excitation energies of the intermediate states contributing to the $0\nu\beta\beta$ transition.

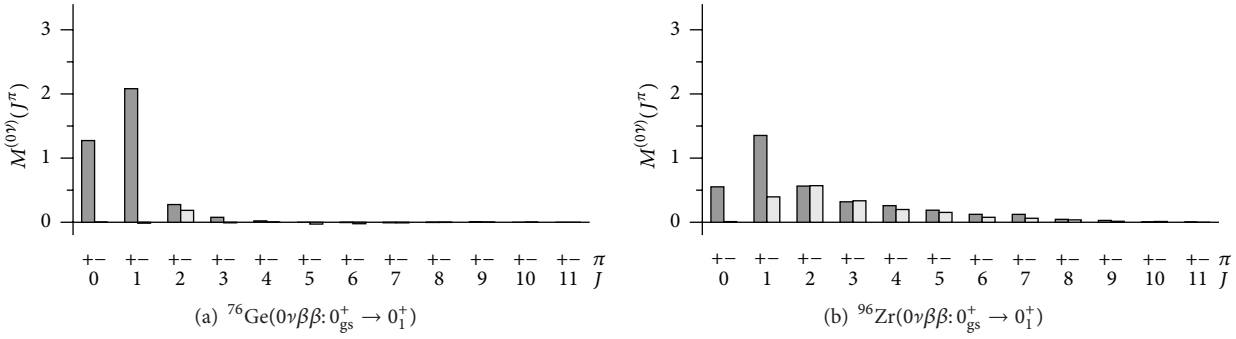

FIGURE 3: Multipole decomposition of the l-NME for the nuclei ^{76}Ge and ^{96}Zr corresponding to the $0^+_{gs} \rightarrow 0^+_1$ decay transitions.

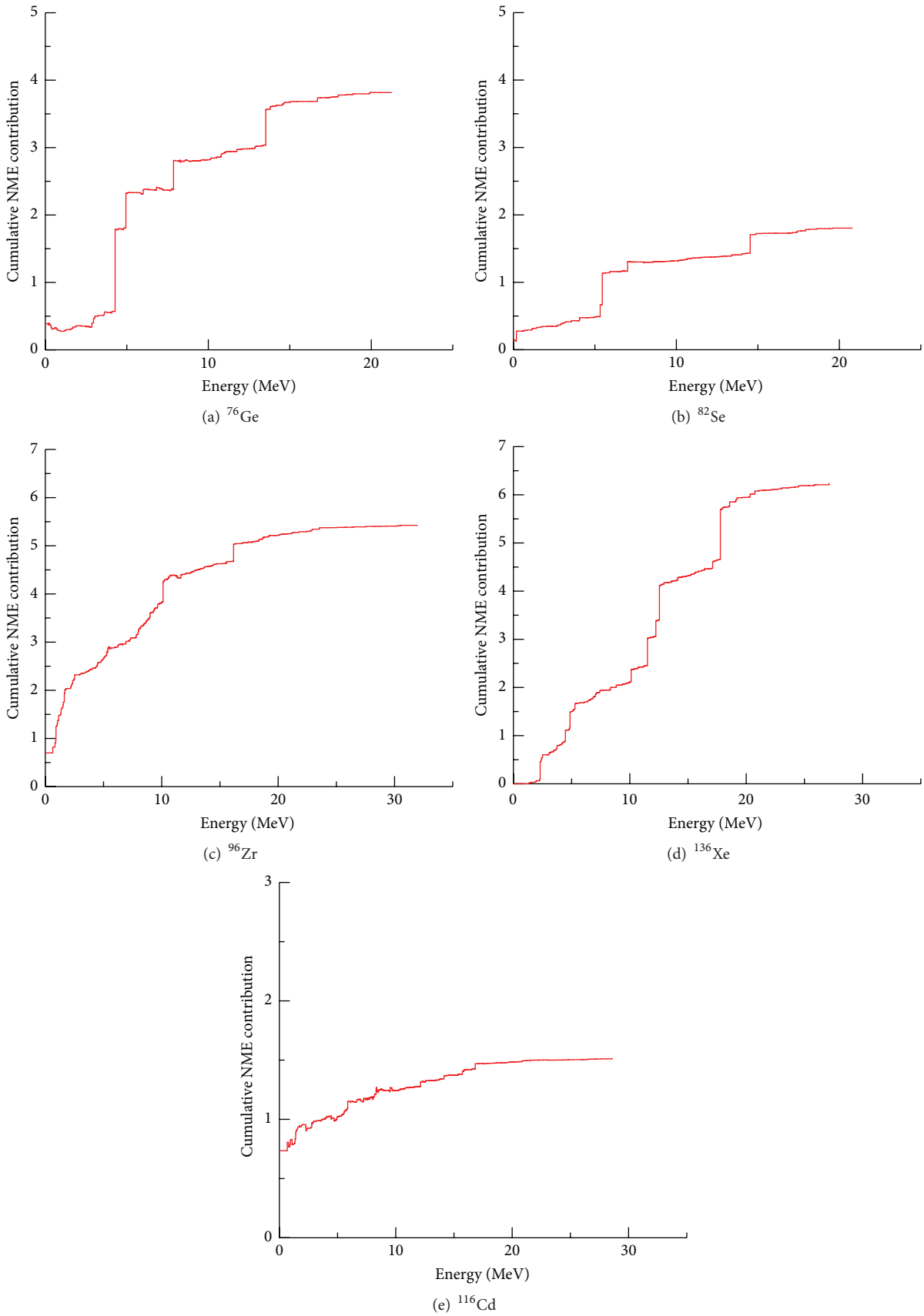

FIGURE 4: Cumulative values of the computed l-NMEs corresponding to the $0^+_{gs} \rightarrow 0^+_1$ decay transitions for the nuclear systems A = 76, 82, 96, 116, and 136. The horizontal axis gives the excitation energies of the intermediate states contributing to the $0\nu\beta\beta$ transition.

Table 1: Most important multipoles and intermediate states contributing to the ground-state-to-ground-state $0\nu\beta\beta$ decays mediated by the light neutrino exchange. Columns E give the energies (in MeVs) and multipoles of the intermediate states. Multipoles are organized from left to right in terms of their importance, the most important being on the left. Columns labeled C give the corresponding NME contributions. Last two numbers in each C column give the summed contribution and the percentual part which the displayed states give to the total multipole strength. The percentage inside the parenthesis gives the fraction with which the displayed states contribute to the total NME.

Nucleus	$E(2^-)$	C	$E(1^-)$	C	$E(2^+)$	C	$E(1^+)$	C	$E(3^-)$	C
	0.22	0.748	5.87	0.155	0.51	0.166	0.00	0.344	0.30	0.189
			6.32	0.058	1.87	0.056	4.09	0.199	0.92	0.148
			7.00	0.077	3.04	0.094	4.48	0.148	6.77	0.056
			7.16	0.064	3.62	0.108	4.94	0.578	6.85	0.053
^{76}Ge			8.27	0.190	4.81	0.058	10.80	−0.053	11.63	0.062
			11.04	0.084	7.73	0.054	11.75	−0.109	12.07	−0.053
			12.03	0.165			13.52	−0.522		
			16.70	0.158						
		0.748		0.635		0.556		0.668		0.454
		79% (11%)		83% (10%)		77% (9%)		88% (10%)		70% (7%)
Nucleus	$E(2^-)$	C	$E(2^+)$	C	$E(1^-)$	C	$E(3^-)$	C	$E(1^+)$	C
	0.00	0.510	0.65	0.137	5.27	0.116	0.07	0.140	0.19	0.264
			1.73	0.065	6.85	0.065	0.82	0.138	3.16	0.095
			2.22	0.051	7.98	0.134			4.07	0.065
			3.56	0.084	9.79	0.083			4.55	0.105
^{82}Se			4.05	0.052	12.25	0.065			5.32	0.559
			4.93	0.054	17.41	0.070			7.01	−0.253
									14.53	−0.396
		0.510		0.442		0.393		0.278		0.439
		81% (11%)		81% (9%)		76% (8%)		57% (6%)		92% (9%)
Nucleus	$E(1^-)$	C	$E(2^-)$	C	$E(3^-)$	C	$E(2^+)$	C	$E(4^+)$	C
	1.75	0.056	0.92	0.498	1.35	0.151	0.64	0.150	1.05	0.099
	2.28	0.063	2.21	0.065	2.35	0.051	1.63	0.114	1.68	0.071
	2.52	0.150	3.75	0.050	7.77	0.064			5.69	0.064
	4.46	0.050	4.43	0.052	11.36	−0.091				
^{96}Zr	5.04	0.077	8.53	0.057						
	5.27	0.209	8.77	−0.056						
	8.65	0.060								
	11.33	0.061								
		0.728		0.666		0.175		0.265		0.234
		83% (16%)		96% (15%)		31% (4%)		59% (6%)		69% (5%)
Nucleus	$E(1^-)$	C	$E(2^+)$	C	$E(4^+)$	C	$E(3^+)$	C	$E(2^-)$	C
	3.12	0.307	0.90	0.192	1.32	0.158	1.33	0.202	1.76	0.205
	4.41	0.109	2.10	0.154	2.26	0.097	1.68	0.076	2.85	0.147
	6.68	0.091	11.68	0.082			7.43	0.152	5.52	−0.061
	11.15	0.117	11.97	−0.070			7.76	−0.173	10.17	0.219
^{100}Mo	16.72	0.058							10.93	−0.194
	20.26	−0.060								
	23.90	−0.060								
		0.562		0.359		0.255		0.257		0.316
		70% (11%)		62% (7%)		53% (5%)		54% (5%)		72% (6%)

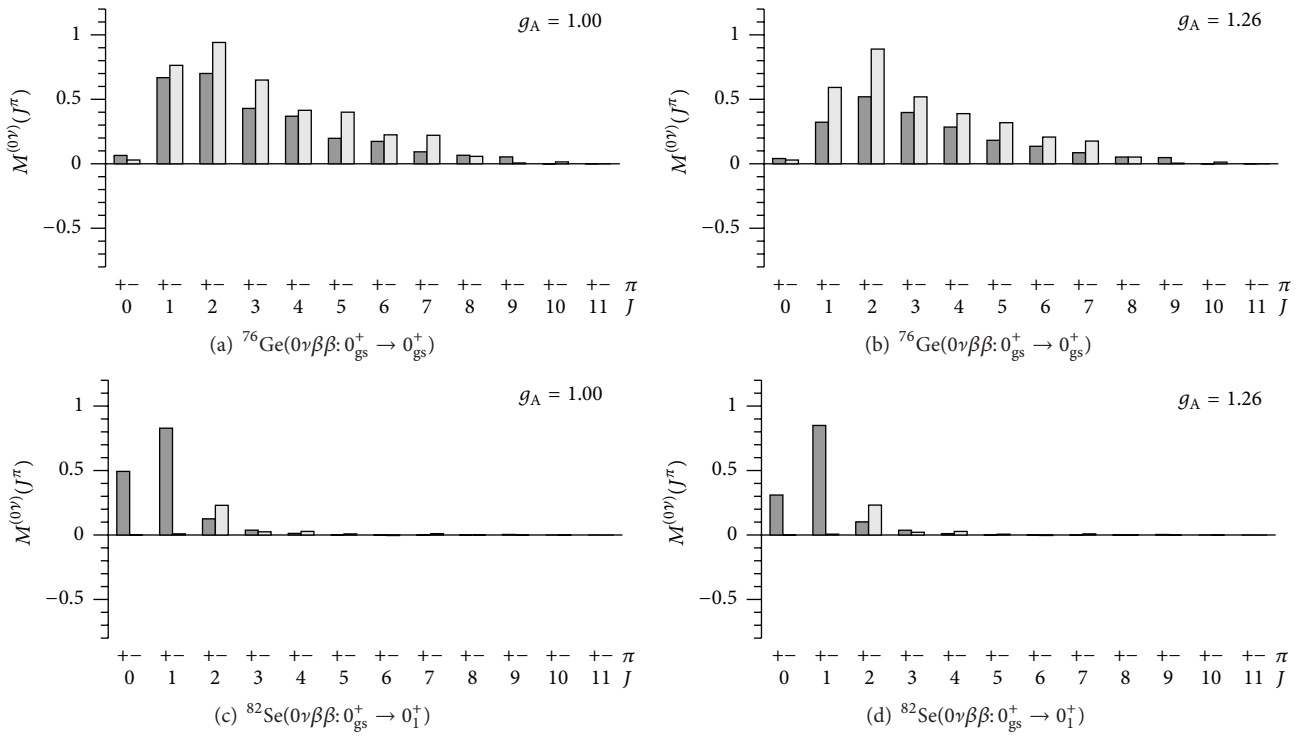

FIGURE 5: Multipole decompositions for the ground-state-to-ground-state decay of the nucleus ^{76}Ge ((a) and (b) panels) and for the ground-state-to-excited-state decay of the nucleus ^{82}Se ((c) and (d) panels). The value $g_A = 1.00$ was used for (a) and (c) panels and the value $g_A = 1.26$ for (b) and (d) panels.

the level structures found in all intermediate odd-odd nuclei considered in this work. This is due to the general feature of odd-odd nuclei: the extremely high density of states even at low energies. This high density of nuclear states becomes a problem, not only for the pnQRPA, but for any other nuclear many-body approach, including the nuclear shell model. The reason for this is that even small perturbations in the two-body interaction matrix elements tend to change the ordering of the levels at random. For this reason the spectra of the odd-odd intermediate nuclei are not a very good measure of the reliability of the calculations but, instead, a better way is to adjust the model parameters in such a way that the transition rates of some other known processes, for example, single or $2\nu\beta\beta$ decays, can be reproduced by the theory and this is the philosophy which we have followed in this work.

3.2. Ground-State-to-Excited-State Decays. Let us then consider $0^+_{gs} \to 0^+_1$ transitions mediated by the light neutrino exchange. In Figures 3(a) and 3(b) we have plotted the multipole decomposition of the l-NMEs corresponding to the $A = 76$ and 96 nuclear systems. The multipole distributions for the excited-state transitions are greatly different from those corresponding to the ground-state transitions. Usually there is only a couple of multipoles, 0^+ and 1^+, which give by far the largest contribution to the NMEs. In this sense the excited-state transitions are more simple than the ground-state transitions. Typical example is the nucleus ^{76}Ge, displayed in Figure 3(a). One nucleus deviating from this trend is ^{96}Zr which is presented in Figure 3(b). Its multipole distribution resembles somewhat more those shown for the ground-state decays in Figures 1(a) and 1(b). Most of this differing behaviour can be traced back to the one-phonon structure of the final 0^+_1 excited state in the nucleus ^{96}Mo. The 0^+_1 final states in this work are modeled as one-phonon basic QRPA excitations for the daughter nuclei ^{96}Mo and ^{116}Sn. Rest of the final states are modeled as two-quadrupole-phonon states. Nucleus ^{96}Zr is an exceptional case since the 0^+_1 state in ^{96}Mo has a relatively low excitation energy and thus boasts rather strong collective features. This is why the excited-state transition has a wide multipole distribution and is greatly enhanced.

Again we can divide nuclei into different groups by considering the shapes of their total cumulative sum distributions. For $0^+_{gs} \to 0^+_1$ transitions via light neutrino exchange, we can differentiate two types of nuclei. *Type 1*: nuclei belonging to type 1 are ^{76}Ge, ^{82}Se, ^{124}Sn, ^{130}Te, and ^{136}Xe. Typical examples of this type, ^{76}Ge, ^{82}Se, and ^{136}Xe, are shown in Figures 4(a), 4(b), and 4(d). Characteristic feature of this type is that there exist only few energy states which give most of the total matrix element producing a staircase-like structure as seen in the panels. For example, for ^{76}Ge there seems to be only five such energy states. *Type 2*: nuclei belonging to this type are ^{96}Zr, ^{100}Mo, ^{110}Pd, and ^{116}Cd. Typical examples of this type are ^{96}Zr and ^{116}Cd shown in Figures 4(c) and 4(e). Characteristic feature of type 2 is that a large number of intermediate states give

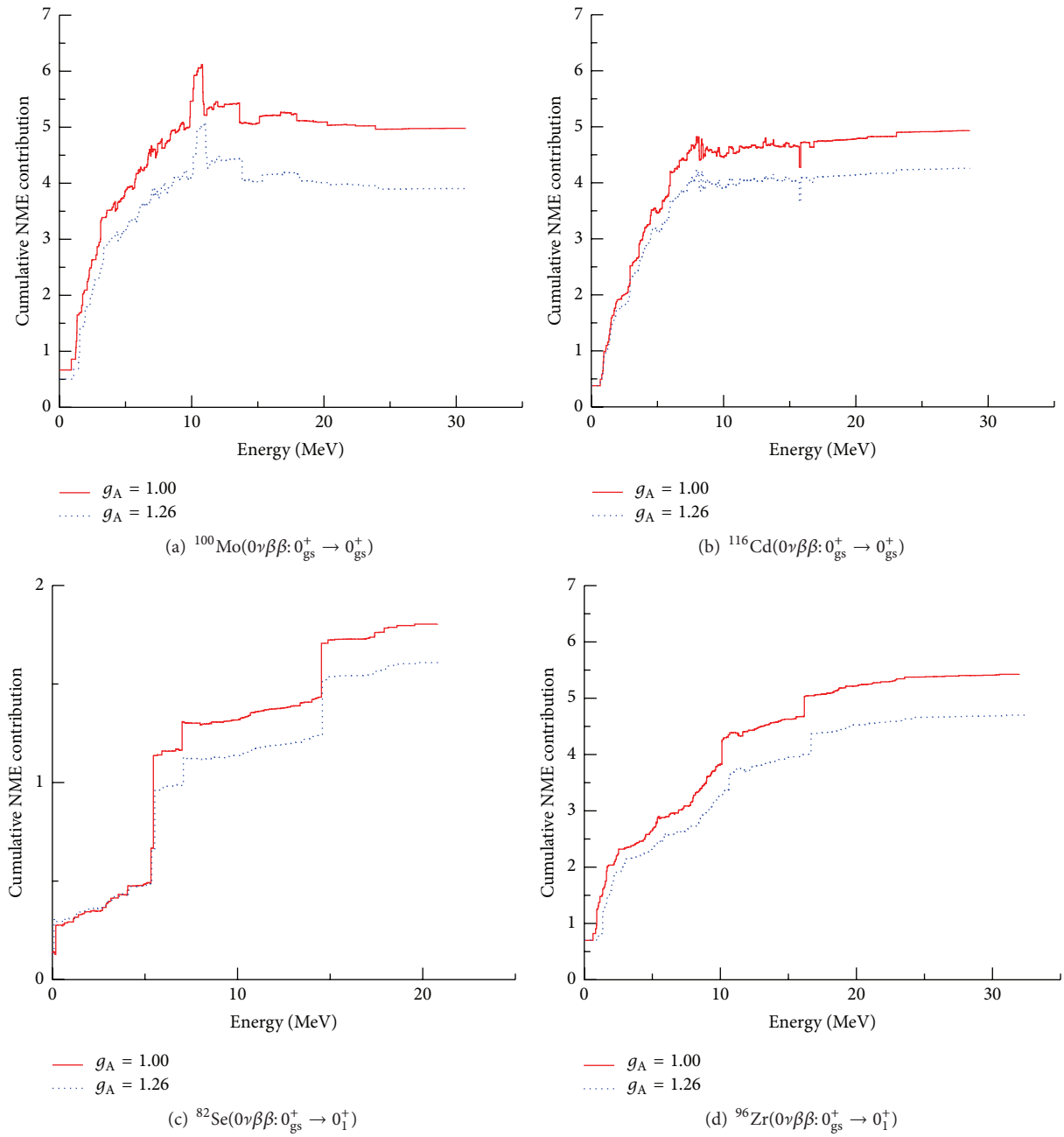

FIGURE 6: Cumulative values of the l-NMEs for ground-state-to-ground-state decays of the nuclei ^{100}Mo and ^{116}Cd ((a) and (b) panels), and for the ground-state-to-excited-state decays of the nuclei ^{82}Se and ^{96}Zr ((c) and (d) panels). The horizontal axis gives the excitation energies of the intermediate states contributing to the $0\nu\beta\beta$ transition. Two different values for the axial coupling were used as indicated in the panels.

important contributions to the NMEs. In case of ^{116}Cd, panel (e), around 50% of the total NME comes from transitions through the ground state of the intermediate nucleus. The other 50% is distributed rather evenly on the interval 0–20 MeV.

Using the multipole decompositions, we extracted the most important multipole components contributing to the light neutrino mediated $0^+_{gs} \to 0^+_1$ decay transitions. These most important components were then again divided into contributions coming from different energy levels of the $0\nu\beta\beta$ intermediate nucleus. These contributions are collected into Table 4 for $A = 76$–116 systems and into Table 5 for $A = 124$–136 systems. Again we notice that often only a few intermediate states give the largest contribution to the dominant multipoles 1^+ and 0^+. Extreme case is the nucleus ^{116}Cd for which the dominant intermediate ground state gives 81% of the total 1^+ strength. Combining this with the fact that 1^+ is by far the largest multipole component, we get a rather good approximation for the total NME by considering just a single virtual transition through the 1^+ ground state

Table 2: Most important multipoles and intermediate states contributing to the ground-state-to-ground-state $0\nu\beta\beta$ decays mediated by the light neutrino exchange. Columns E give the energies (in MeVs) and multipoles of the intermediate states. Multipoles are organized from left to right in terms of their importance, the most important being on the left. Columns labeled C give the corresponding NME contributions. Last two numbers in each C column give the summed contribution and the percentual part which the displayed states give to the total multipole strength. The percentage inside the parenthesis gives the fraction with which the displayed states contribute to the total NME.

Nucleus	$E(1^-)$	C	$E(2^-)$	C	$E(1^+)$	C	$E(3^-)$	C	$E(2^+)$	C
	2.95	0.130	0.82	0.387	0.00	0.938	1.14	0.118	0.33	0.244
	3.19	0.106	2.47	0.091	4.70	−0.062	1.64	0.128	0.95	0.087
	3.44	0.221	2.63	0.163	9.61	0.153	1.91	0.080	8.68	0.061
	3.81	0.426	5.94	0.107	9.75	−0.146	3.07	0.053	8.73	0.075
	4.52	0.126	8.88	0.161	10.22	0.079	3.61	0.075	9.00	0.061
	9.11	0.109	9.54	−0.256	15.16	−0.316	5.33	0.066	9.07	0.053
^{110}Pd					16.30	0.256	8.08	0.167	9.16	0.199
							8.37	−0.051	9.30	−0.366
							8.45	0.052		
							8.68	0.275		
							9.11	−0.468		
		1.118		0.653		0.903		0.496		0.414
		77% (13%)		68% (7%)		96% (10%)		60% (6%)		55% (5%)
Nucleus	$E(1^-)$	C	$E(3^-)$	C	$E(2^-)$	C	$E(1^+)$	C	$E(3^+)$	C
	3.61	0.223	1.72	0.081	1.84	0.065	0.00	0.378	0.90	0.158
	4.47	0.099	2.30	0.053	2.93	0.287	8.37	−0.102	1.40	0.068
	5.37	0.118	2.79	0.051	7.56	0.075	9.51	0.087	3.89	0.057
	5.87	0.140	7.24	0.104	8.31	0.246	10.74	−0.083		
	8.61	0.102			8.34	0.103	11.20	0.081		
	23.07	0.071			8.45	−0.262	13.75	0.080		
^{116}Cd					9.69	−0.051	13.79	−0.087		
							15.73	−0.363		
							15.83	0.440		
							16.51	−0.082		
							16.83	0.092		
		0.753		0.289		0.463		0.439		0.284
		72% (15%)		65% (6%)		106% (9%)		102% (9%)		76% (6%)
Nucleus	$E(1^-)$	C	$E(1^+)$	C	$E(2^+)$	C	$E(2^-)$	C	$E(3^-)$	C
	1.68	0.522	0.00	0.690	0.23	0.157	0.52	0.271	0.36	0.050
	4.82	0.089	1.00	−0.067	0.60	0.083	1.82	0.225	0.49	0.110
	6.54	0.082	2.56	0.252	1.06	0.056	4.55	0.051	1.95	0.150
	9.57	0.059	3.31	0.153	2.15	0.066	7.60	0.057	9.67	0.086
	10.74	0.159	6.72	−0.130	7.11	0.055	7.66	−0.064	9.70	0.062
^{124}Sn	14.07	0.065	9.51	0.098			10.20	0.183	9.82	−0.087
	14.46	−0.099	13.09	−0.112			10.35	−0.094	12.64	−0.053
	14.83	−0.058								
	16.36	−0.087								
	18.05	−0.067								
		0.664		0.884		0.417		0.629		0.318
		55% (8%)		95% (11%)		53% (5%)		89% (8%)		49% (4%)

of the intermediate nucleus ^{116}In. As for the ground-state-to-ground-state decays in some cases notable contributions are coming from high excitation energies, well above 10 MeV. There are high-energy contributions in case of 1^+ multipole for all nuclei, and in the cases of 2^- and 2^+ multipoles for ^{130}Te and ^{136}Xe.

3.3. Effects of g_A on the Intermediate-State Contributions. As mentioned earlier, we have used in this work the quenched value for the axial vector coupling $g_A = 1.00$. Next we shall briefly examine how our results will change if we increase the value of g_A from the quenched value 1.00 to the bare value 1.26. The effect of this amplification of the axial coupling

Table 3: Most important multipoles and intermediate states contributing to the ground-state-to-ground-state $0\nu\beta\beta$ decays mediated by the light neutrino exchange. Columns E give the energies (in MeVs) and multipoles of the intermediate states. Multipoles are organized from left to right in terms of their importance, the most important being on the left. Columns labeled C give the corresponding NME contributions. Last two numbers in each C column give the summed contribution and the percentual part which the displayed states give to the total multipole strength. The percentage inside the parenthesis gives the fraction with which the displayed states contribute to the total NME.

Nucleus	$E(1^-)$	C	$E(2^+)$	C	$E(3^-)$	C	$E(2^-)$	C	$E(3^+)$	C
	4.22	0.200	0.04	0.066	0.16	0.055	0.61	0.335	0.02	0.074
	4.72	0.060	0.51	0.052	0.58	0.140	4.02	0.060	2.37	0.063
	6.21	0.078	2.93	0.084	3.97	0.052	4.55	0.101	6.22	0.078
	6.44	0.059	3.97	0.053	10.04	0.061	4.89	−0.070	6.77	−0.065
	8.07	−0.084	6.77	0.050			10.14	0.136	9.82	−0.062
	8.30	0.151					10.57	−0.056	10.27	−0.057
^{128}Te	8.98	0.068					11.55	0.058		
	10.69	−0.052								
	11.12	0.182								
	17.48	−0.079								
	19.19	−0.100								
		0.484		0.305		0.308		0.564		0.154
		69% (8%)		52% (5%)		58% (5%)		120% (10%)		33% (3%)
Nucleus	$E(1^-)$	C	$E(2^+)$	C	$E(3^-)$	C	$E(3^+)$	C	$E(2^-)$	C
	4.18	0.184	0.13	0.054	0.84	0.113	0.10	0.056	0.97	0.277
	5.72	0.059	3.16	0.089			0.36	0.052	10.25	0.061
	6.27	0.059	4.70	0.064			2.60	0.056	11.33	−0.100
	8.56	0.096	10.49	−0.065			6.35	0.063		
^{130}Te	11.26	0.115	10.57	0.145			6.83	0.054		
	17.77	−0.062	10.97	−0.088			12.31	0.059		
	19.51	−0.079	16.44	0.150			12.41	−0.065		
			16.54	−0.132						
		0.373		0.216		0.113		0.166		0.237
		61% (7%)		40% (4%)		25% (2%)		39% (3%)		56% (5%)
Nucleus	$E(2^+)$	C	$E(3^+)$	C	$E(1^-)$	C	$E(2^-)$	C	$E(4^+)$	C
	1.59	0.033	1.35	0.033	6.65	0.141	4.86	0.188	2.34	0.032
	2.26	0.038	2.39	0.054	7.32	0.044	7.42	0.068	2.44	0.061
	2.50	0.037	4.81	0.050	10.31	0.053			4.43	0.031
	5.29	0.067	8.27	0.035					4.76	0.049
^{136}Xe	6.57	0.033	9.99	0.027					7.67	0.034
	7.05	0.027	10.65	−0.027					9.10	0.045
	14.11	0.087							9.65	−0.038
	14.25	−0.085								
		0.238		0.172		0.238		0.256		0.214
		62% (7%)		53% (5%)		76% (7%)		85% (7%)		71% (6%)

strength on the NMEs is demonstrated in Figure 5 where we have plotted the multipole decompositions for nuclei ^{76}Ge and ^{82}Se calculated with both values of the axial coupling $g_A = 1.00$ and $g_A = 1.26$. In case of the ground-state-to-ground-state decays, the 1^+ multipole changes rather fast when the axial coupling is increased from 1.00 to 1.26. This happens mainly due to the changing of the g_{pp} parameter (for each g_A value, the parameter g_{pp} is adjusted in such a way that the measured $2\nu\beta\beta$ rate is reproduced). The 1^+ multipole contribution is very sensitive to the value of g_{pp}. We can see from Figures 5(a) and 5(b) that for $g_A = 1.00$ the 1^+ component is among the five most important multipoles, while for $g_A = 1.26$ it is not. Some of the higher multipoles change also somewhat, but not so rapidly. Ground-state-to-excited-state transitions proceed mainly through the 0^+ and 1^+ multipole channels. We see from Figures 5(c) and 5(d) that increasing the value of g_A affects mostly the 0^+ component.

Figure 6 displays the total cumulative sum distributions for ground-state-to-ground-state decays of the nuclei ^{100}Mo and ^{116}Cd (panels (a) and (b)), and for ground-state-to-excited-state decays of the nuclei ^{82}Se and ^{96}Zr (panels (c) and (d)). Axial coupling values $g_A = 1.00$ and $g_A = 1.26$

Table 4: Most important multipoles and intermediate states contributing to the ground-state-to-excited-state $0\nu\beta\beta$ decays mediated by the light neutrino exchange. Columns E give the energies (in MeVs) and multipoles of the intermediate states. Multipoles are organized from left to right in terms of their importance, the most important being on the left. Columns labeled C give the corresponding NME contributions. Last two numbers in each C column give the summed contribution and the percentual part which the displayed states give to the total multipole strength. The percentage inside the parenthesis gives the fraction with which the displayed states contribute to the total NME.

Nucleus	$E(1^+)$	C	$E(0^+)$	C
	0.00	0.390	2.86	0.053
	2.95	0.062	4.28	1.204
	4.94	0.501		
^{76}Ge	7.87	0.435		
	13.52	0.522		
		1.909		1.256
		92% (50%)		99% (33%)

Nucleus	$E(1^+)$	C	$E(0^+)$	C
	0.19	0.149	5.45	0.471
	5.32	0.179		
	7.01	0.145		
^{82}Se	14.53	0.274		
		0.746		0.471
		90% (41%)		96% (26%)

Nucleus	$E(1^+)$	C	$E(2^-)$	C	$E(2^+)$	C	$E(0^+)$	C	$E(1^-)$	C
	0.00	0.700	0.92	0.283	0.64	0.122	5.37	0.033	2.28	0.032
	7.81	0.051	9.66	0.057	1.63	0.180	6.64	0.025	2.52	0.080
	8.99	0.058			5.37	0.035	7.32	0.037	4.46	0.026
^{96}Zr	11.65	0.065			6.92	0.027	8.02	0.036	5.27	0.068
	16.17	0.354					10.12	0.396	11.33	0.026
							12.00	0.013		
		1.228		0.340		0.364		0.540		0.232
		91% (23%)		60% (6%)		65% (7%)		98% (10%)		59% (4%)

Nucleus	$E(1^+)$	C	$E(0^+)$	C
	9.42	0.090	9.01	0.076
	13.62	0.079	9.55	0.150
	14.31	0.072		
^{100}Mo	15.12	0.063		
		0.303		0.226
		65% (40%)		77% (30%)

Nucleus	$E(1^+)$	C	$E(0^+)$	C
	0.00	0.308	10.26	0.165
	10.22	0.059		
	13.73	0.083		
^{110}Pd	14.56	0.055		
	15.16	0.072		
		0.577		0.165
		76% (53%)		70% (15%)

Nucleus	$E(1^+)$	C
	0.00	0.735
^{116}Cd		0.735
		81% (48%)

Table 5: Most important multipoles and intermediate states contributing to the ground-state-to-excited-state $0\nu\beta\beta$ decays mediated by the light neutrino exchange. Columns E give the energies (in MeVs) and multipoles of the intermediate states. Multipoles are organized from left to right in terms of their importance, the most important being on the left. Columns labeled C give the corresponding NME contributions. Last two numbers in each C column give the summed contribution and the percentual part which the displayed states give to the total multipole strength. The percentage inside the parenthesis gives the fraction with which the displayed states contribute to the total NME.

Nucleus	$E(1^+)$	C	$E(0^+)$	C				
	0.00	0.101	2.70	0.667				
	0.66	0.433	4.60	0.088				
	1.00	0.146	7.35	0.567				
	2.25	0.051						
	2.56	0.227						
^{124}Sn	3.31	0.664						
	6.72	0.289						
	7.91	0.424						
	13.09	0.473						
	13.86	0.161						
		2.968		1.322				
		94% (44%)		94% (19%)				
Nucleus	$E(1^+)$	C	$E(0^+)$	C	$E(2^-)$	C	$E(2^+)$	C
	0.25	0.390	7.40	0.719	0.97	0.340	0.41	0.019
	1.50	0.082	8.35	0.631	5.07	0.073	0.59	0.047
	2.32	0.097			17.26	0.106	1.83	0.017
	2.76	0.134			18.95	0.083	2.80	0.043
	4.53	0.064					4.70	0.024
	5.59	0.338					4.86	0.027
^{130}Te	7.57	0.592					5.18	0.033
	14.66	0.065					6.27	0.016
	15.01	0.259					6.75	0.051
	15.07	0.773					9.10	0.032
	15.39	0.089					10.57	0.045
							17.87	0.026
							23.14	0.024
		2.882		1.351		0.602		0.390
		95% (41%)		99.6% (19%)		79% (9%)		65% (6%)
Nucleus	$E(1^+)$	C	$E(0^+)$	C	$E(2^-)$	C	$E(2^+)$	C
	2.30	0.366	12.24	0.317	2.50	0.060	4.86	0.204
	3.06	0.050	12.54	0.712	4.86	0.056	18.58	0.083
	3.75	0.066			5.29	0.113	20.34	0.059
	4.46	0.226			8.34	0.053		
^{136}Xe	10.12	0.232			14.11	0.054		
	11.52	0.565						
	17.12	0.137						
	17.78	1.031						
		2.675		1.029		0.335		0.346
		93% (43%)		101% (16%)		53% (5%)		67% (6%)

were adopted. We notice from the figures that increasing the axial coupling strength shifts the distributions downwards. This is especially true for the higher energy parts. Despite this fact, the overall shapes of the cumulative sum distributions do not change much and the same classification of nuclei into different categories according to their cumulative distribution shapes seems to hold also for larger values of g_A.

4. Conclusions

In this paper we have extended our previous work [17] on the ground-state-to-ground-state $0\nu\beta\beta$ decay transitions. In the present work we have concentrated our studies on the intermediate contributions to the NMEs involved in the light neutrino mediated $0\nu\beta\beta$ decay. We have calculated the intermediate state multipole decompositions of the NMEs and extracted the most important multipole components. Cumulative sums of the NMEs were calculated to investigate the important energy regions contributing to the $0\nu\beta\beta$ transitions. Finally, the most important multipole components were divided into contributions coming from the virtual transitions through the individual states of the $0\nu\beta\beta$ intermediate nuclei. An extensive tabulation of these important intermediate states were given for all the nuclei considered in this paper.

We have done these computations by using realistic two-body interactions and single-particle bases. All the appropriate short-range correlations, nucleon form factors, and higher-order nucleonic weak currents are included in our present results.

We found in the calculations that often there exists only a few relevant intermediate states which collect most of the strength corresponding to a given multipole. We also found that there exists a single-state dominance in the important 2^- components related to the ground-state decays of nuclei ^{76}Ge, ^{82}Se and perhaps also for ^{96}Zr.

Competing Interests

The authors declare that they have no competing interests.

Acknowledgments

This work has been partially supported by the Academy of Finland under the Finnish Centre of Excellence Programme 2012–2017 (Nuclear and Accelerator Based Programme at JYFL).

References

[1] J. Suhonen and O. Civitarese, "Weak-interaction and nuclear-structure aspects of nuclear double beta decay," *Physics Report*, vol. 300, no. 3-4, pp. 123–214, 1998.

[2] F. T. Avignone, S. R. Elliott, and J. Engel, "Double beta decay, Majorana neutrinos, and neutrino mass," *Reviews of Modern Physics*, vol. 80, no. 2, pp. 481–516, 2008.

[3] J. D. Vergados, H. Ejiri, and F. Šimkovic, "Theory of neutrinoless double-beta decay," *Reports on Progress in Physics*, vol. 75, no. 10, p. 106301, 2012.

[4] J. Maalampi and J. Suhonen, "Neutrinoless double β^+/EC decays," *Advances in High Energy Physics*, vol. 2013, Article ID 505874, 18 pages, 2013.

[5] M. Kortelainen, O. Civitarese, J. Suhonen, and J. Toivanen, "Short-range correlations and neutrinoless double beta decay," *Physics Letters, Section B: Nuclear, Elementary Particle and High-Energy Physics*, vol. 647, no. 2-3, pp. 128–132, 2007.

[6] F. Šimkovic, G. Pantis, J. D. Vergados, and A. Faessler, "Additional nucleon current contributions to neutrinoless double β decay," *Physical Review C*, vol. 60, no. 5, Article ID 055502, 14 pages, 1999.

[7] J. Suhonen and O. Civitarese, "Review of the properties of the $0\nu\beta^-\beta^-$ nuclear matrix elements," *Journal of Physics G: Nuclear and Particle Physics*, vol. 39, no. 12, Article ID 124005, 2012.

[8] P. Vogel, "Nuclear structure and double beta decay," *Journal of Physics G: Nuclear and Particle Physics*, vol. 39, no. 12, p. 124002, 2012.

[9] J. Barea, J. Kotila, and F. Iachello, "Nuclear matrix elements for double-β decay," *Physical Review C*, vol. 87, no. 1, Article ID 014315, 2013.

[10] A. Neacsu and S. Stoica, "Study of nuclear effects in the computation of the $0\nu\beta\beta$ decay matrix elements," *Journal of Physics G: Nuclear and Particle Physics*, vol. 41, no. 1, Article ID 015201, 2014.

[11] J. Engel, "Uncertainties in nuclear matrix elements for neutrinoless double-beta decay," *Journal of Physics G: Nuclear and Particle Physics*, vol. 42, no. 3, Article ID 034017, 2015.

[12] F. Šimkovic, A. Faessler, V. Rodin, P. Vogel, and J. Engel, "Anatomy of the $0\nu\beta\beta$ nuclear matrix elements," *Physical Review C: Nuclear Physics*, vol. 77, no. 4, Article ID 045503, 2008.

[13] M. T. Mustonen and J. Engel, "Large-scale calculations of the double-β decay of ^{76}Ge, ^{130}Te, ^{136}Xe, and ^{150}Nd in the deformed self-consistent Skyrme quasiparticle random-phase approximation," *Physical Review C*, vol. 87, Article ID 064302, 2013.

[14] F. Šimkovic, V. Rodin, A. Faessler, and P. Vogel, "$0\nu\beta\beta$ and $2\nu\beta\beta$ nuclear matrix elements, quasiparticle random-phase approximation, and isospin symmetry restoration," *Physical Review C*, vol. 87, no. 4, Article ID 045501, 9 pages, 2013.

[15] V. A. Rodin, A. Faessler, F. Šimkovic, and P. Vogel, "Assessment of uncertainties in QRPA $0\nu\beta\beta$-decay nuclear matrix elements," *Nuclear Physics A*, vol. 766, pp. 107–131, 2006.

[16] D.-L. Fang, A. Faessler, V. Rodin, and F. Šimkovic, "Neutrinoless double-β decay of deformed nuclei within quasiparticle random-phase approximation with a realistic interaction," *Physical Review C*, vol. 83, no. 3, Article ID 034320, 8 pages, 2011.

[17] J. Hyvärinen and J. Suhonen, "Nuclear matrix elements for $0\nu\beta\beta$ decays with light or heavy Majorana-neutrino exchange," *Physical Review C*, vol. 91, no. 2, Article ID 024613, 12 pages, 2015.

[18] P. Pirinen and J. Suhonen, "Systematic approach to β and $2\nu\beta\beta$ decays of mass $A = 100 - 136$ nuclei," *Physical Review C*, vol. 91, no. 5, Article ID 054309, 2015.

[19] H. Ejiri, N. Soukouti, and J. Suhonen, "Spin-dipole nuclear matrix elements for double beta decays and astro-neutrinos," *Physics Letters B*, vol. 729, pp. 27–32, 2014.

[20] J. Menéndez, D. Gazit, and A. Schwenk, "Chiral two-body currents in nuclei: Gamow-Teller transitions and neutrinoless double-beta decay," *Physical Review Letters*, vol. 107, no. 6, Article ID 062501, 5 pages, 2011.